685

[redacted]

RECORD COPY

SNPO-C

WANL-TME-1193

June 1965

MASTER

Westinghouse Astronuclear Laboratory

UPGRADING OF SINGLE ELEMENT HOT HYDROGEN CORROSION TESTING
(Title Unclassified)

DISTRIBUTION OF THIS DOCUMENT IS UNLIMITED

RECORD COPY

[redacted]

DISCLAIMER

DISCLAIMER

Portions of this document may be illegible in electronic image products. Images are produced from the best available original document.

19

~~CONFIDENTIAL~~
~~RESTRICTED DATA~~
~~Atomic Energy Act 1954~~

Astronuclear Laboratory

WANL-TME-1193

June 1965

MASTER

~~GROUP I~~
~~Excluded From Automatic Downgrading and Declassification~~

65

UPGRADING OF SINGLE ELEMENT HOT HYDROGEN CORROSION TESTING
(Title Unclassified)

by

W. D. Pouchot
J. W. H. Chi
Fluid Flow Laboratory
Experimental Engineering Department

Classification cancelled (~~or changed to~~)
by authority of
by TIC, date SEP 11 1973

Approved By:

E. A. DeZubay, Manager
Fluid Flow Laboratory

~~INFORMATION CATEGORY~~
~~CONFIDENTIAL R. D.~~
~~Authorized Classifier~~ 6-30-65 ~~Date~~

SPECIAL REREVIEW FINAL DETERMINATION	Reviewer	Class.	Date
Class: U	KAW	U	4-19-82

~~CONFIDENTIAL~~
~~RESTRICTED DATA~~
~~Atomic Energy Act 1954~~

SUMMARY

An analytical examination has been made of the Westinghouse practices and equipment used in hot hydrogen single element electrical corrosion testing of fuel elements. Means are suggested by which both the operational and reactor-like simulation aspects of these tests may be improved both at presently required testing temperatures and higher.

Two major areas of concern investigated were arcing from the hot end chuck (electrode) to the test element and simulation of a reactor-like temperature distribution in the test sample.

A program of development of the electrical chucking is now underway and is to be continued. A solution to the electrical part of the problem is to grasp the test element firmly. This approach creates gas leakage and/or relative expansion problems which need further work to obtain a complete solution.

Simulation of a reactor-like temperature distribution has two aspects. The first is determining to a better degree of accuracy the present electrical test distribution. The second is that of tailoring the distribution to a given reactor-like profile. Additional voltage and temperature measurements are suggested as an aid in clearing up the first aspect of the the problem. Conceptual designs involving cold end electrical chuck position, changes in furnace thermal radiation shielding, and guard heaters are suggested as a part of the program to improve the second aspect of the problem. Procurement of an additional power supply is recommended to allow unimpeded implementation of the guard heater approach.

In addition to arcing and reactor-like temperature simulation, an operational problem which looms at this time is a marginal thermal capacity in the exit gas heat exchanger and transition piece. With improvement in these three problem areas, the furnace and its auxiliary equipment appear to be capable of much higher temperature service than that currently required.

TABLE OF CONTENTS

TABLE OF CONTENTS (CONTINUED)

LIST OF FIGURES

I. INTRODUCTION

This report is for the purpose of presenting and discussing a number of proposals by which corrosion tests on single fuel elements in hot flowing hydrogen may be improved. These discussions center on the A-2 furnace design and auxiliary equipment. The A-2 furnaces are the workhorses for single element corrosion tests at WANL.

The A-2 high temperature hydrogen corrosion furnace consists of a horizontally-mounted, water-cooled pressure vessel, a heat exchanger for cooling exhaust gases, and a direct-current power supply. Heating is achieved by electrical resistance heating of the fuel element.

The furnace includes flow and pressure controllers to:

1) maintain the desired pressure at the hot-end of the furnace (560 psia),
2) provide a constant flowrate of 500 SCFM of hydrogen, and
3) monitor helium flow used to pressurize the vessel.

A cross-section view of the furnace proper is shown in Figure 1.

The pressure vessel is fitted with five viewports and optical pyrometers to permit the determination of fuel element surface temperatures.

At the present time surface temperatures are regularly measured at only three of the five ports. These locations correspond to distances measured along the test element from the cold end of 16-1/2-inches, 38-1/2-inches, and 49-3/4-inches.

During a test, a fuel element is installed in the center of the furnace, held at each end by graphite chucks. The desired hydrogen flowrate is first introduced through the coolant channels while a helium atmosphere is maintained outside the

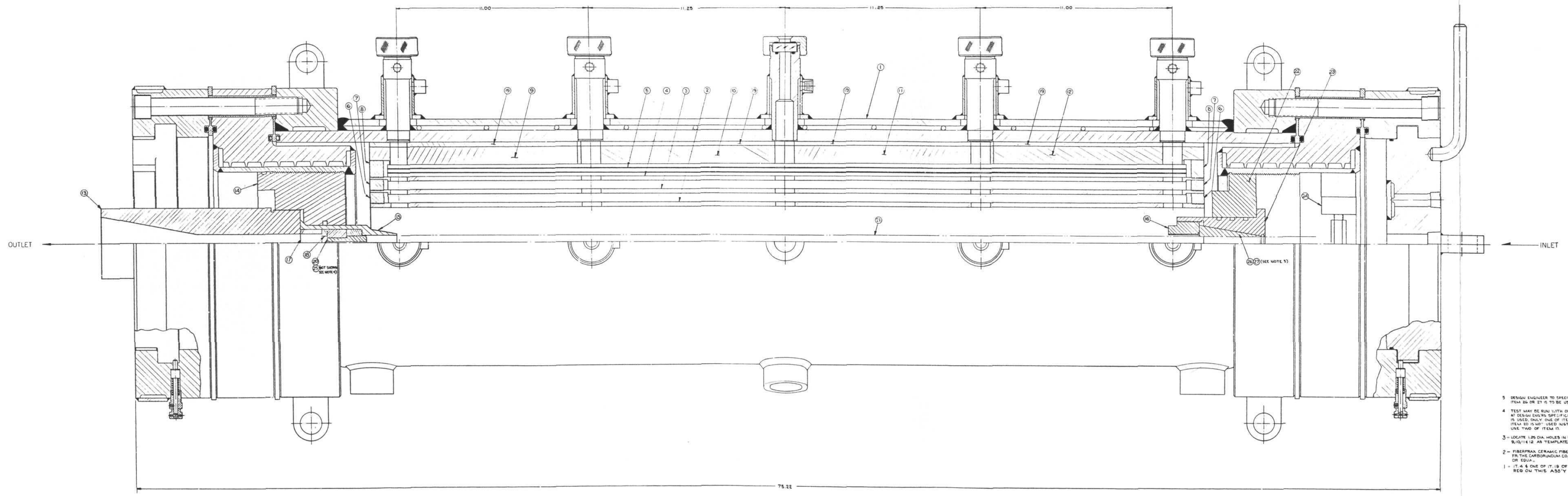

5 DESIGN ENGINEER TO SPECIFY WHETHER ITEM 26 OR 27 IS TO BE USED.

4 TEST MAY BE RUN WITH OR WITHOUT ITEM 20 AT DESIGN ENG'RS SPECIFICATION - IF ITEM 20 IS USED, ONLY ONE OF ITEM 17 IS REQ'D. IF ITEM 20 IS NOT USED INSTALL ITEM 25 AND USE TWO OF ITEM 17.

3 - LOCATE 1.25 DIA. HOLES IN IT. 19 USING ITS. 9, 10, 11 & 12 AS TEMPLATES

2 - FIBERFRAX CERAMIC FIBER-FELT TYPE XV FR. THE CARBORUNDUM CO., PERTH AMBOY, N.J. OR EQUAL

1 - IT. 4 & ONE OF IT. 19 OF THIS DWG. NOT REQ ON THIS ASS'Y

QTY REQ	NOTE	ITEM NO	NOMENCLATURE OR DESCRIPTION	CODE IDENT NO	PART OR IDENTIFYING NO	MATERIAL	SPECIFICATION
1	NOTE 5	27	CHUCK		710J477H18		
1	NOTE 5	26	CHUCK		710J477H17		
1	NOTE 4	25	STOP		710J477H15		
1		24	SHOE ASS'Y		710J477G02		
1		23	SLIDING CHUCK		710J477H03		
1		22	RETAINING RING		710J477H02		
REF		21	FUEL ELEMENT				
1	NOTE 4	20	SUPPORT BLOCK		710J477H012	GRAPHITE	COM'L
4	2 & 3	19	INSULATION 36.00 OF 50X12 CD			FIBERFRAX BLANKET	COM'L
1		18	STOP		710J477G03		
2		17	SPACER		710J477H06		
1		16	LOCK NUT		710J477G04		
1		15	CHUCK		710J477H05		
1		14	RETAINING RING		710J477H04		
1		13	DIFFUSER		710J477H07		
1		12	INSULATION		975D894H04		
1		11	INSULATION		975D894H03		
1		10	INSULATION		975D894H02		
1		9	INSULATION		975D894H01		
2		8	RING		944C464H03		
2		7	RING		944C464H02		
2		6	RING		944C464H01		
1		5	SHIELD		975D638H01		
1		4	SHIELD		928F508H03		
1		3	SHIELD		928F508H02		
1		2	SHIELD		928F508H01		
1	NOTE 1	1	FURNACE ASSEMBLY		934J506G01		

LIST OF MATERIALS

DRAWN DEVINE
WESTINGHOUSE ELECTRIC CORPORATION
Astronuclear Laboratory, PITTSBURGH, PA.
GENERAL ASSEMBLY WATER COOLED FURNACE
CODE IDENT NO 14683 | SIZE J | DWG NO 934J506
751357-A
SCALE 1/1

Figure 1

A-2 Furnace Cross-Section

fuel element.* After the flow is stabilized, power is then supplied in steps until a specified test element surface temperature (determined at the viewport, 38-1/2-inches from the cold end) is attained. Thereafter, this temperature is maintained for a specified length of time by adjusting the power input.

II. DISCUSSION OF SINGLE ELEMENT TESTING EXPERIENCE

A. Operational Experience and Difficulties

1. Present operating temperature levels:

Current operating levels are designated as conditions 1A, 1B and 1C. These conditions are identified on the basis of a surface temperature achieved at a location 49-3/4-inches from the cold end of the fuel element. The 49-3/4-inch location is approximately 1/4 to 1/2-inch from the beginning of the hot end electrical chuck. Because of perturbations which can be introduced by the presence of the chuck, control of the test is maintained on the basis of a corresponding set of temperatures at a location 38-1/2-inches from the cold end plus overall electrical power input.

The flows, surface temperatures and approximate power levels for each of these conditions are given in Table I.

Operating times at a given condition are measured in multiples of 5 minutes up to 20 minutes. For example, tests at condition 1B for 5 minutes or 20 minutes are designated 1B5 and 1B20, respectively. A test in which the test element remains in the furnace continuously but in which the power is supplied over say two discrete 5 minute

---

* The corrosion resistance on the internal coolant passages and the hot end faces of the fuel element are the principle items on which information is obtained.

Table I

Corrosion Test Operating Levels

Condition	49-3/4-Inch Surface Temperature °R	Hydrogen Flow Rate lb/sec	Approximate Power Input KW
1A	4600	0.04426	870
1B	4460	0.04426	830
1C	4320	0.04426	770

intervals, with cooling of the element in between, is designated a 1B5+5 test. At the present time, quality control tests are commonly 1B5+5 and 1B20. Test run time for quality control tests is limited, at the present, to the 5+5 duration in the case of restarts and +20 in the case of continuous runs. By so limiting these test times two major operational problems with the furnace are largely avoided. These major operational problems are (1) "shrinkage" of the hot end electrical chuck with time and resultant arcing, and (2) sudden and complete breakage of the test element.

The sudden and complete breaking of a fuel element is commonly called an "abort". The causes of "aborts" have not been clearly defined. Aside from the obvious observation that certain elements behave differently from their fellows, theories hold that "aborts" are due to (1) complete element cracking from thermal stresses at the hot end chuck position, (2) bore coat cracking from thermal stresses followed by rapid corrosion at the hot end, and (3) melting of the bore coat caused by the high maximum internal temperatures because of the increased radial gradient present in the higher temperature tests.

Other operational problems of a more minor or non-repetitive nature have been noted. Among these is arcing between the electrically hot, thermally cold, end of the furnace and electrical ground, the slow cooldown rate of the furnace, and occasionally the exhaust gas heat exchanger and exhaust pipe temperatures approach or exceed design limits. Aside from these discrepancies the operational aspects of the (A-2) furnace at present test conditions is quite satisfactory.

2. Possible future higher temperature levels:

It is probable that sometime in the future that higher temperature performance will be a goal of NERVA development. Such a possibility should not be ignored in any upgrading work on hot hydrogen tests. The level of the higher temperature goals is, of course, open at this time. Assume for discussion that the eventual goal will move upwards in 500°R intervals by at least 1500°R or that future goals will be $+500^{\circ}$R, $+1000^{\circ}$R and $+1500^{\circ}$R above present levels. These increments correspond, approximately, to maximum observed element surface temperatures fo $4960 \pm 150^{\circ}$R, $5460 \pm 150^{\circ}$R, and $5960 \pm 150^{\circ}$R.

Substantial numbers of tests have been run which correspond to the $+500^{\circ}$R increase in temperature level. More specifically 21 tests have been carried out with measured maximum element surface temperatures between 4800°R and 5000°R. In addition, five tests with measured surface temperatures between 5000°R and 5200°R have been conducted.

The nominal running time for the $+500^{\circ}$R (approximately) tests was five minutes. About 1/3 of the elements tested remained intact for the full five minutes. Tests of elements in the same furnace for quality control purposes, at current temperature levels in the same calendar time period, showed 90% element survival.* Increasing the temperature level $+500^{\circ}$R increased "failures" from about 10% to 67%.

*Substantial improvements have been made in element manufacture and coating processes since mid-1964 when these failure rates were observed.

While the increase in "failures" is the most noticeable feature of the +500°R tests, other problems are noted. Most important of these is that the exhaust gas cooler outlet temperature ran very close to or in excess of the acceptable limits of 860°R on almost all of the runs. Other problems recorded were, over pressure limit "cutout" of the system, and exceeding of pyrometer calibration temperatures. While no information is specifically recorded in the test logs, the problem of hot electrical chuck shrinkage and subsequent arcing which is present in longer time tests at current temperatures will, undoubtedly, be made worse by higher temperatures.

Aside from the troubles previously recountered, the operational aspects of the A-2 furnace at the +500°R condition is satisfactory.

B. Simulation of Reactor Temperature Distribution

1. Experimental observations:

To reduce the difficulties of interpretation of electrical corrosion test results in terms of reactor operation, it is obviously desirable that the corrosion tests should duplicate, as closely as practical, reactor flows and temperature distributions. Areas of principle concern are the internal and external flows through and around a single fuel element and the simulation of reactor-like axial and radial temperature distributions throughout the fuel element. The topic of discussion here is the axial and radial temperature distribution of a single fuel element under electrical test.

Under reactor conditions heat input rates in the fuel element as a function of length approximate a chopped cosine distribution which is unlikely to be duplicated by the electrical resistance of the test element. Fortunately, the electrical resistance of elements under actual corrosion test can be inferred to be lower at the hot end of the element than in the middle or cold end.[1,2] Such a hot end resistivity decrease results in an electrical test axial power distribution that tends, in a gross fashion, towards a reactor-like distribution.

In Reference 1, indirect calculations of the hot end electrical resistivity indicated it to be as much as 50% below that at the cold end. Resistivity measurements on a fuel element held at a nearly constant temperature (axially) as reported in Reference 2 indicate that this 50% difference is excessive and that the difference should be in the order of 5 to 10%. Since neither set of data is a result of a direct measurement of electrical resistivity under corrosion test conditions, they cannot be considered as definitive of the axial power distribution for single element corrosion tests without further substantiation.

To investigate the likely effect of changes in axial electrical resistivity on the temperature distribution in an element undergoing corrosion testing, hypothetical resistance patterns were assumed. These patterns are shown as lines A, B, and C in Figure 2, a plot of electrical resistivity as a function of temperature. These lines were selected to cover by calculation a wide range of hot to cold end resistivity variation and not to imply that any particular hypothetical pattern is correct. This approach has the advantage that the calculations are not tied to a particular set of elements of a particular stage of fuel element evolution.

The radial temperature gradient is more pronounced in the electrical corrosion test than in an actual reactor.

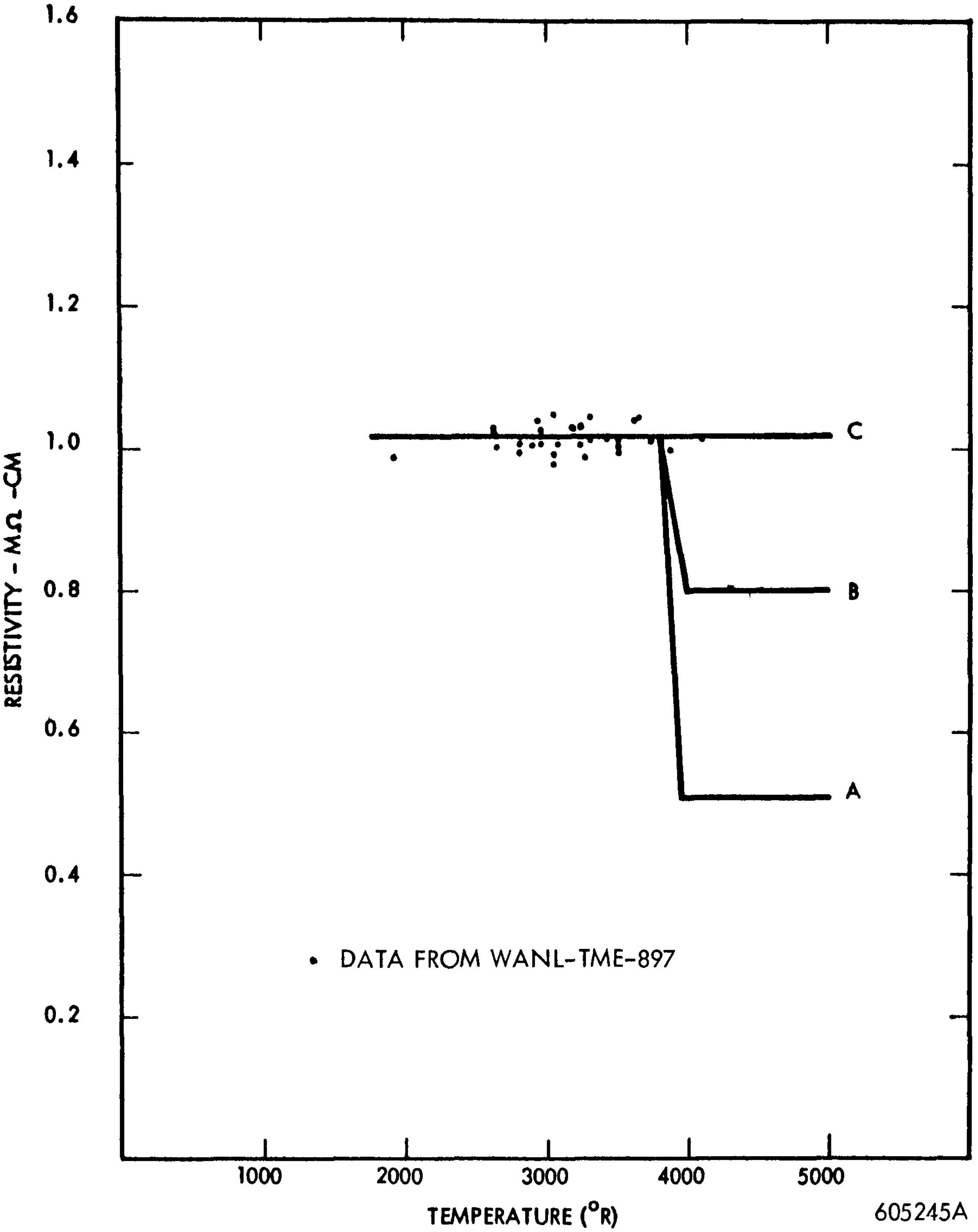

Figure 2

Element Electrical Resistivity

To simulate reactor-like conditions the radial gradient in the element must be controlled. The difference between maximum internal temperature and surface temperature is caused by the heat loss at the surface of the element. In the apparatus as presently constructed, it is a strong function of surface temperature. For example a measured difference at 4455°R surface temperature is 405°R but increases to 645°R at 4595°R surface temperature. The major factor here is that the difference is proportional to the heat loss from the surface which in turn is proportional to the fourth power of the surface temperature, neglecting convective losses. Neglecting the convective losses in this apparatus is a doubtful procedure except for exposition purposes because of the presence of helium and helium flows over the element. The convective losses may amount to as much as 15 to 20% of the total surface loss at the hot end under present testing conditions. A correlation of measured radial temperature differences is presented in Figure 3. This is a plot of the referred measured maximum temperature difference between internal web temperature and surface temperature at a given axial station against the referred surface heat loss. The correlation is presented as a function of two assumed resistivity patterns (refer to Figure 1 for patterns B and C) because the local electrical heat generated per unit length (q''') is a calculated quantity which depends upon the local resistivity assumed.

Ways to control this surface heat loss are shielding and/or guard heating. On the basis of measurements, the present shielding arrangement in the A-2 furnace is quite ineffective in reducing hot end element surface radiative heat transfer. The reduction from an unshielded condition being on the order of 12%. The problem is

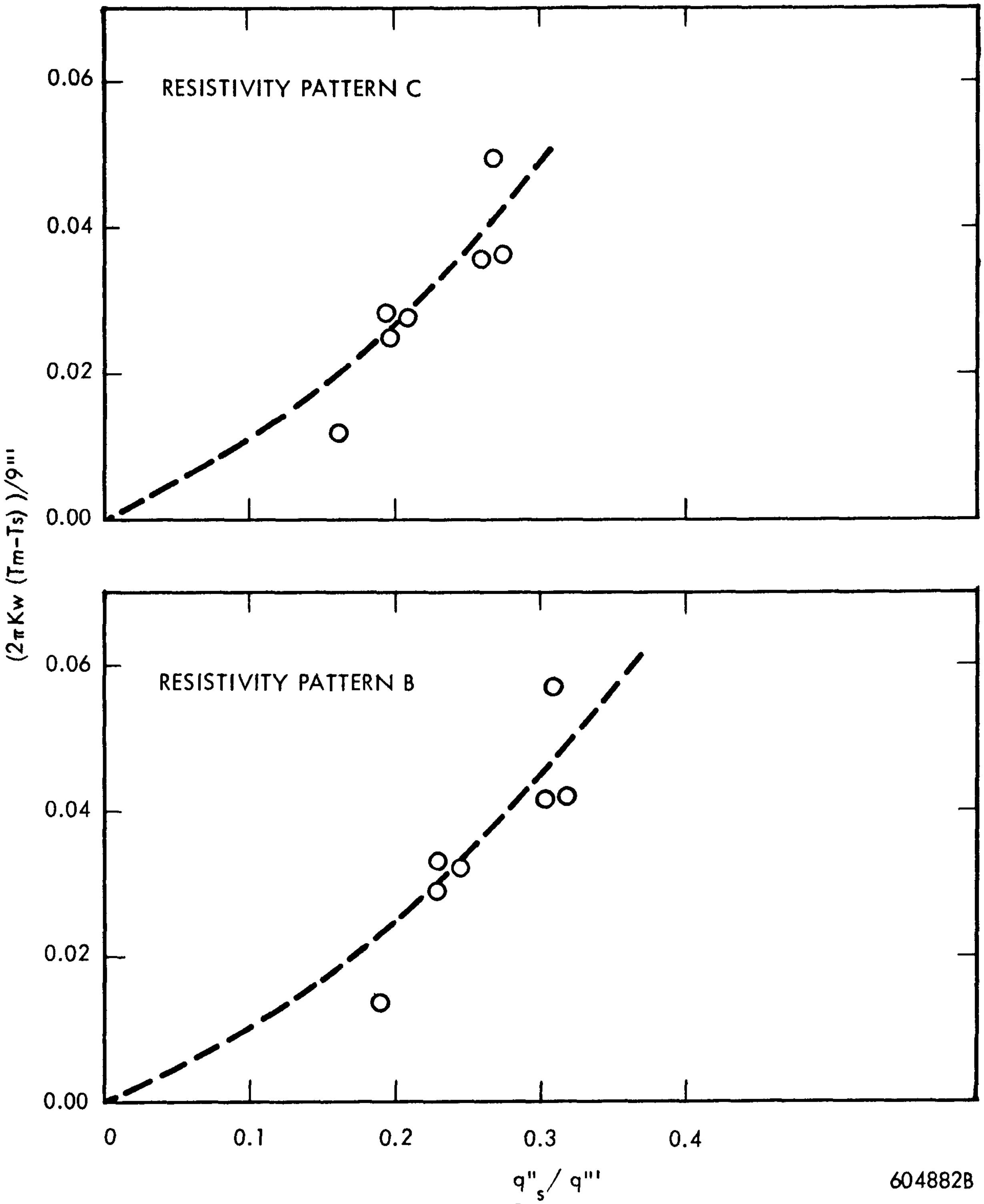

Figure 3

Hot End Radial Temperature Distribution Correlation twofold. First the basic geometry and materials of the primary shields are such that if they behaved ideally, the reduction in radiation flux would be 33% of the unshielded value. This is because the primary shields are of large diameter compared to the element and are made of graphite which has a high emissivity. The relative diameters may be observed in the cross-section drawings of Figure 1 which is approximately to scale. The second half of the problem may also be observed in Figure 4. This is the heavy support structure at the ends of the shield, its close unshielded position next to the end of the furnace, and the heavy cross-section of the three primary shields. If the support structure were a solid piece, all the radiation incident on the last one-inch of the shield could be conducted to insulation covering the body with a thermal drop of only 300°F. The breaks in this support structure undoubtedly contribute a substantial resistance to heat flow but there is also substantially more than 300°F thermal drop available (about 3000°F before the back radiation from the innermost shield becomes large enough to much reduce the element heat loss). While the insulation covering the body introduces a substantial resistance to direct heat flow to the body and water cooling passages, the alternate heat transfer paths of radiation to the water cooled portion of the end of the furnace plus conduction along the inner shields back to the cold end compensate.

2. Corrosion test temperature distribution vs reactor temperature distributions:[5]

a. Background for calculations:

This subject has already been discussed in the preceding section to a certain extent. However, during most

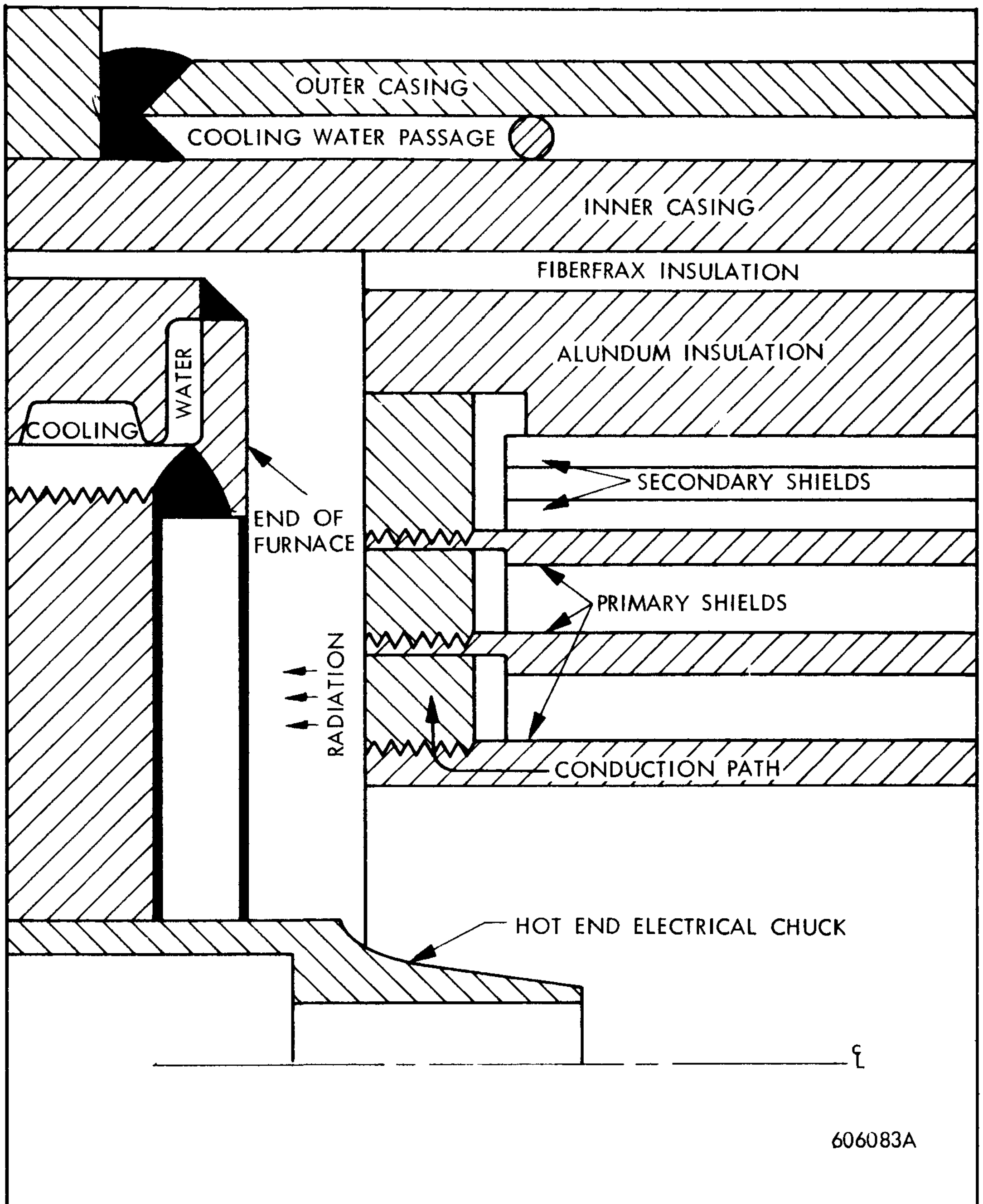

FIGURE 1 PARTIAL SECTION HOT END A-2 FURNACE

Figure 4

Partial Section Hot End A-2 Furnace

tests the surface temperatures are measured at only three locations along the element and except for a few special tests such as presented in the correlation of Figure 3, the internal web temperatures are not measured (because of the difficulties involved). Therefore, to fill the gaps in the observations, calculation is necessary.

These calculations involve a number of assumptions about the local electrical resistivity of the element, the emissivity of the element surface, the effectiveness of the radiation shields, the convective heat transfer to the hydrogen flowing through the elements, the convective heat transfer away from the element surface to the surrounding helium atmosphere, and the thermal conductivity of the element.

The relative importance of errors in assumption in each of these areas in the total heat balance is illustrated in Table II. This table is an approximate breakdown by category of the various total heat rates making up an overall heat balance in the present 1B tests. Obviously, in an overall sense, the controlling terms in a calculation are the electrical heat generation and the heat convected to the hydrogen. Substantial percentage errors in the other heat rate quantities can be tolerated without introducing much overall error. Considerations based on overall values rather than local conditions can, of course, be misleading. For example the radiative surface loss is a more important factor at the hot end than its overall value would indicate. This is illustrated in Table III where the various values are compared per unit of

Table II

Approximate Overall Heat Balance - 1B Test Conditions

Electrical Heat Generation	849 KW
Heat Convected to Hydrogen	706 KW
Element Surface Loss by Radiation	62 KW
Electrode Conduction	49 KW
Element Surface Loss by Convection	32 KW

Table III

49-3/4-Inch Station Heat Rates - 1B Test Conditions

Electrical Heat Generation	14.8 KW/in
Heat Convected to Hydrogen	10.2 KW/in
Element Surface Loss by Radiation	3.9 KW/in
Electrode Conduction	Negligible
Element Surface Loss by Convection	.7 KW/in

length at the 49-3/4-inch length point of the element. This location is approximately 1/2-inches ahead of the beginning of the hot end chuck (electrode). Comparison is made for a calculated 1B test condition assuming an electrical resistivity distribution corresponding to curve "B" of Figure 2. Even at the hot end it is evident that an error in assumed electrical resistivity (generation rate is proportional to the resistivity) or hydrogen convective heat transfer coefficient is more important than the same percentage error in radiative transfer.

Because of the uncertainty in the electrical resistivity distribution of a fuel element under actual test, calculations have been carried out for three hypothetical distributions. These are the lines labelled A, B and C of Figure 2, previously mentioned.

The calculations using the hypothetical resistivity variation respresented by line A (derived on the basis of Reference 1 which was a first indication of this kind of resistivity variations), were carried out by WANL Reactor Analysis using the TOSS-MCAP computer code.[6] For the less extreme hypothetical variations in cold to hot end resistivity as represented by lines B andC, the accuracy of hand calculations was deemed sufficient for the purposes of this report and the calculations carried out accordingly.

For the calculations using resistivities B and C as carried out by hand, the overall heat balance was closed to approximately 2%. The Dittus-Boelter type correlation -

$$\left(N_{Nu}\right)_b = .023\left(N_{Pr}\right)_b^{.4}\left(N_{Re}\right)_b^{.8}\left(\frac{T_b}{T_w}\right)^{-.55}$$

where T_b - is the bulk temperature

T_w - is the wall temperature

and Nusselts, Prandtls, and Reynolds Numbers are based on bulk properties.

- was used to obtain an average coolant channel convective heat transfer coefficient assuming heat flux into the gas from all channels to be the same at any particular axial station.

Surface heat transfer losses by radiation were taken as 82% black-body radiation with no effective back radiation from the surroundings. A discussion of the radiation assumptions is given in Appendix A. Convective heat loss rate from the element surface to the helium surroundings was taken as 120,000 BTU/hr-ft^2. There is a great deal of uncertainty in this number and values from 40,000 BTU/hr-ft^2 to 120,000 BTU/hr-ft^2 can be generated depending upon furnace flow patterns assumed. There is a strong natural convection component in this loss. Fortunately, this particular heat rate is small compared to some of the other heat rates, as has been discussed previously.

Calculations for resistivity patterns B and C are based on average hydrogen flow rate values through the element per coolant channel. The maximum internal web temperatures and the surface temperatures were obtained by superimposing the temperature spread as derived from the correlations of Figure 3 on the calculated average element material temperature at the various axial locations along the element. In the preparation and use of the correlations of Figure 3, the thermal conductivity values for the fuel element were based on actual measured values on fuel elements.[1] Extrapolation of this information to higher temperatures was required.

b. Results of comparison:

Calculated surface temperatures for the three hypothetical resistivity patterns A, B and C are shown as a function of axial length in Figure 5. These values are for a 1B test condition and with the end of the cold end chuck at 4-inches and the beginning of the hot end chuck at 50-1/4-inches along the 52-inch long test element. As can be seen, wide differences in calculated temperatures exist between the three assumed patterns. Pattern B gives a better agreement with test measurements than patterns A and C, although far from ideal. The test values plotted represent the averages and extremals of 30 1B tests selected by chance. The agreement of all the patterns and measurement at the 49-3/4 point is a deliberate result of the calculation procedures.

The comparisons of Figure 5 show how important it is to know the local values of element electrical resistivity as it actually exists in an element under test. They also show the desireability of obtaining experimental surface temperature measurements at more axial stations along a test element.

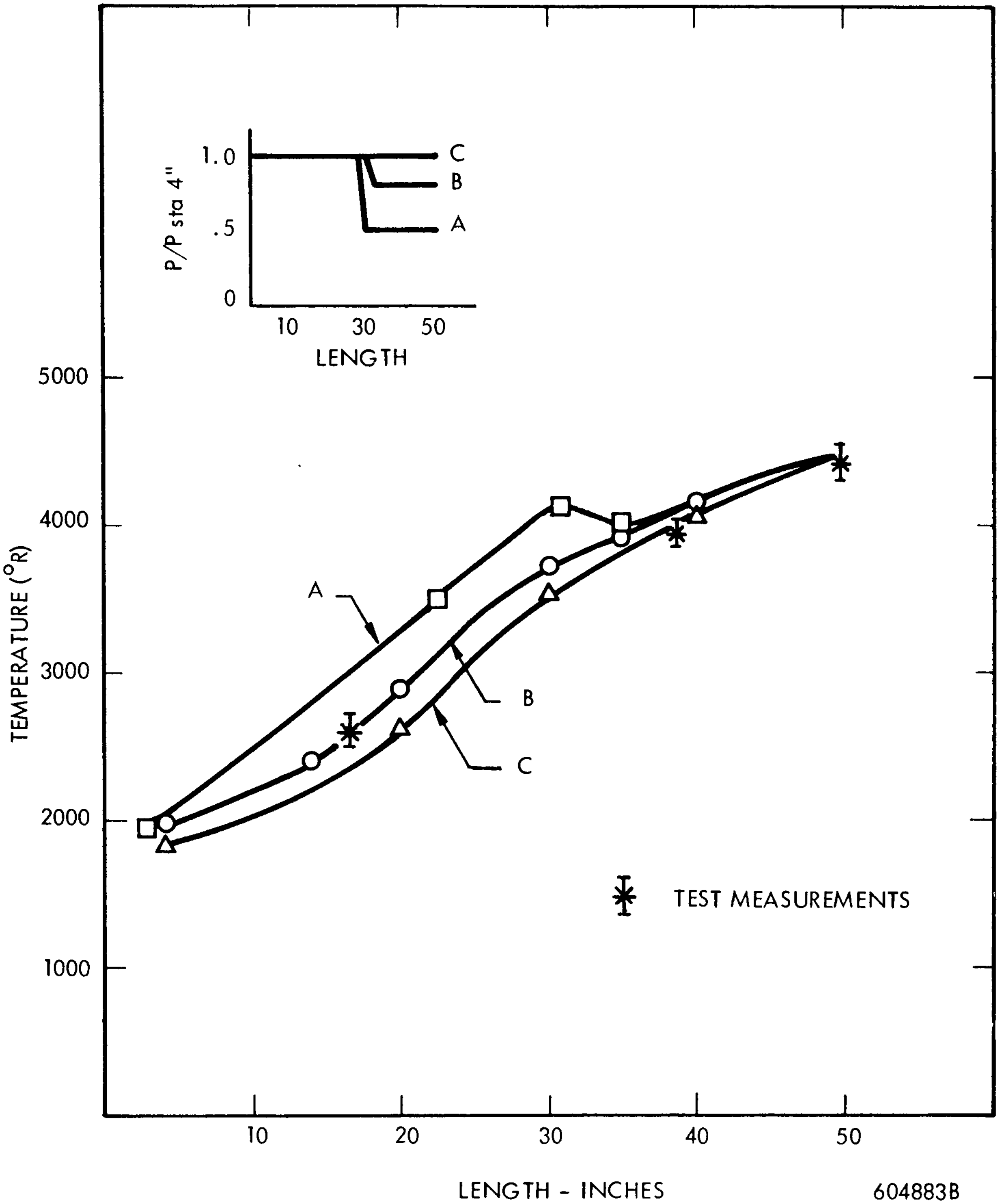

Figure 5

Surface Temperatures - Corrosion Tests

In Figure 6 are shown the maximum corrosion test material temperatures calculated for the same set of conditions as those of Figure 5. Included on this curve are two broken lines representative of fuel element material temperatures during reactor operation.[6] The highest of these reactor lines are temperatures 3 standard deviations (3σ) above nominal maximum. Accepting resistivity pattern B as the most nearly correct of the 3 assumed patterns, it can be seen that the maximum material temperatures during the electrical tests fall between the reactor temperature lines over most of the element length. However, the electrical tests are not consistently either high or low with respect to hypothetical reactor material temperatures over the length of the element. They are a variable scan across reactor conditions axially and also radially at the hot end.

Figure 7 shows the calculated gas temperatures corresponding to the material temperatures of Figures 5 and 6. It is included for completeness.

One of the ways in which the axial temperatures of an electrical test element might be shifted to more nearly correspond to a consistent set of reactor element temperatures is by changing the location of the cold end chuck (electrode). In Figure 8 are plotted two curves. The upper curve labelled "4-inch chuck location" is a replot of curve B from Figure 5. The lower curve labelled "12-inch chuck location" are calculated values for the 1B test condition but with the downstream end of the cold end chuck at 12-inches instead of the

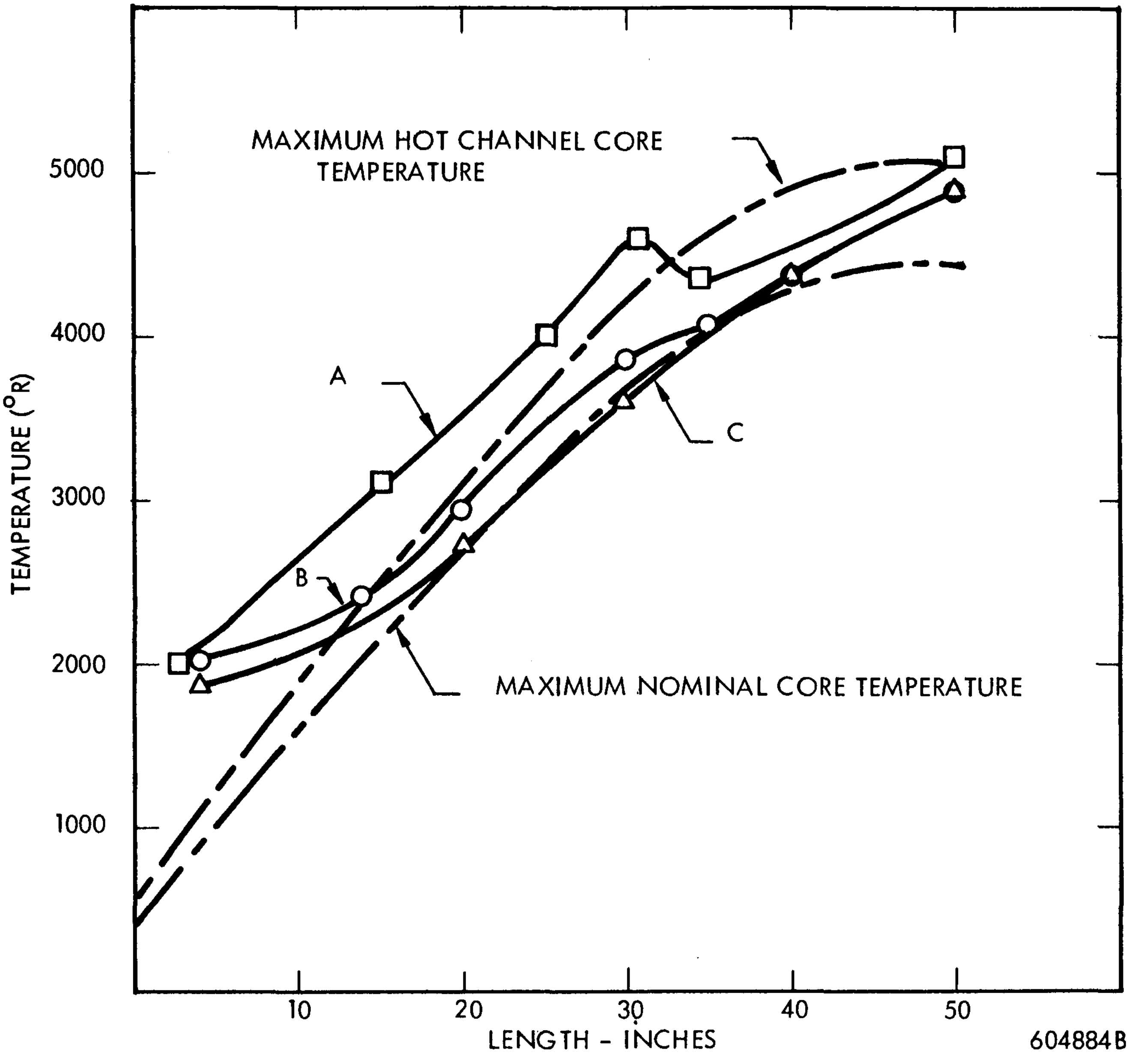

Figure 6

Calculated Maximum Material Temperatures - Corrosion Tests

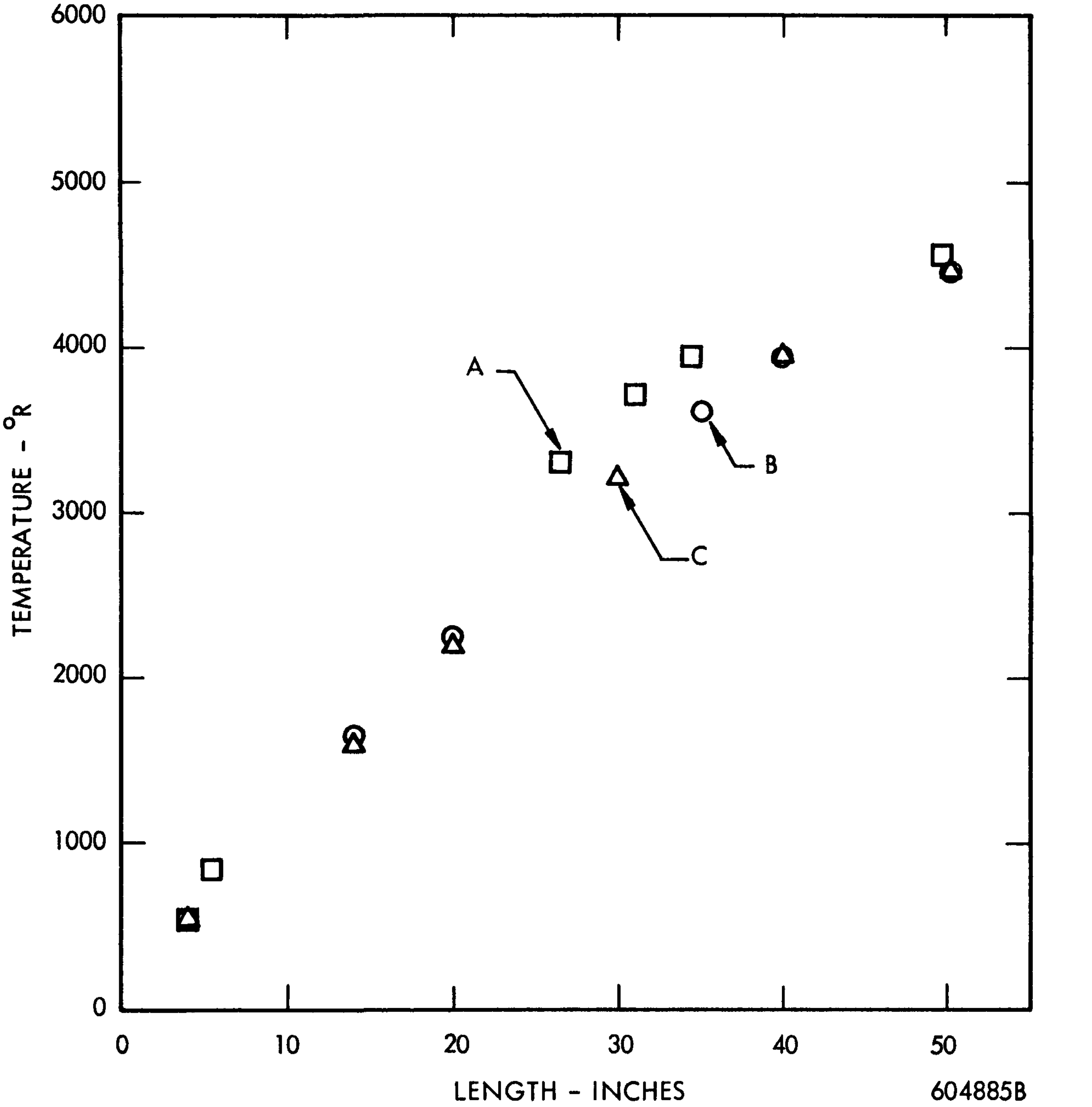

Figure 7

Calculated Gas Temperatures - Corrosion Tests

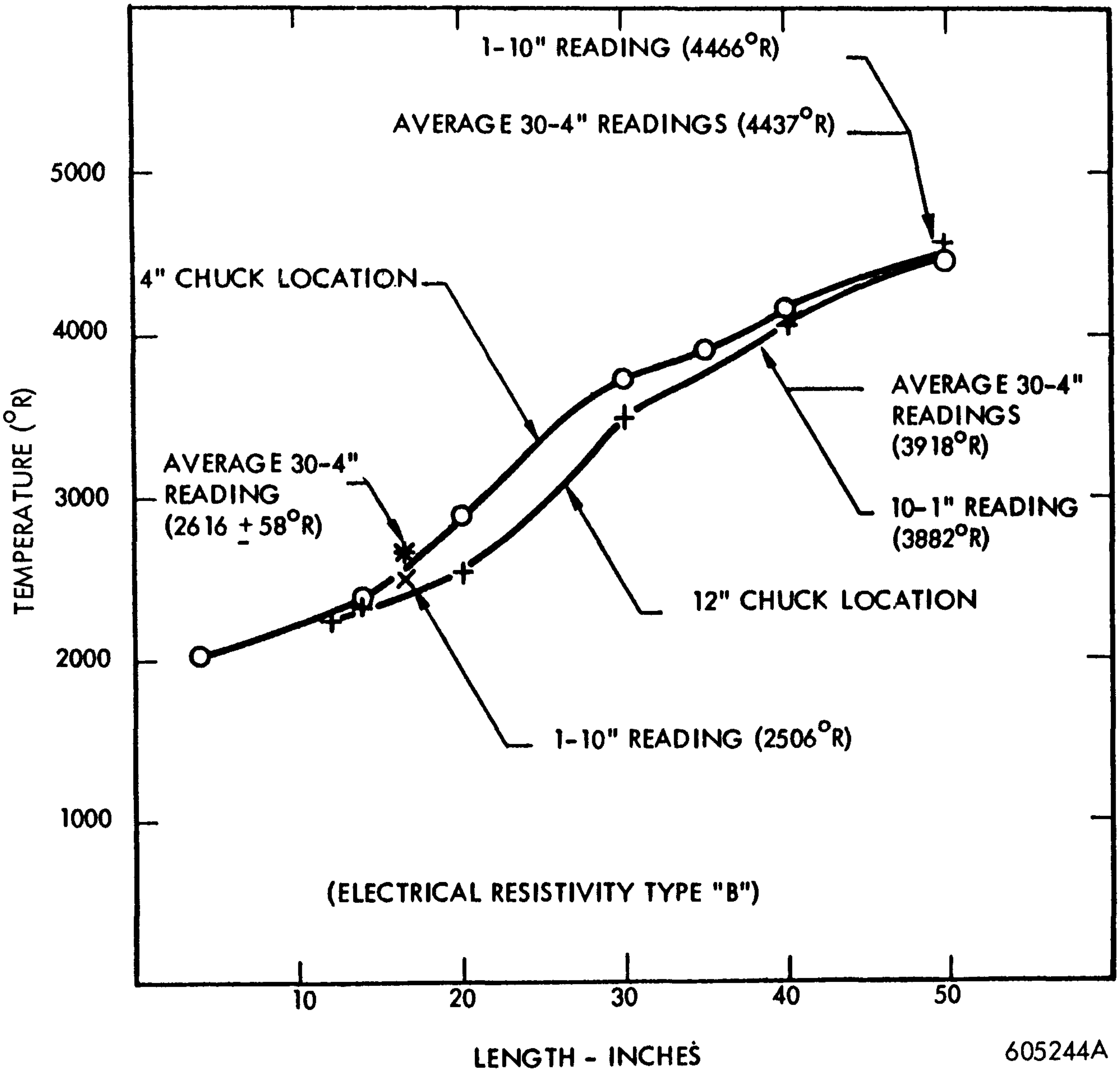

Figure 8

Chuck Position vs Surface Temperatures

standard 4-inches. A comparison with experimental results consisting of the (previously reported) average of 30 - 4-inch readings and one test with a 10-inch cold end chuck location is also shown in Figure 8. The observed shifts in surface temperature are in agreement with the calculated shift. Since the calculated shift is greatest at about 25-inch axial length, measurement of surface temperatures in this region is clearly desirable.

The calculated effect of this shift on maximum material temperature is given in Figure 9; again compared with the two reactor temperature profiles. It would appear that elimination of the radial gradient at the hot end would result in the 12-inch chuck location simulating, rather closely, the reactor "maximum nominal core temperature" elements.

III. PROPOSED A-2 FURNACE CHANGES

The following changes to the A-2 furnace design are proposed as possible means of eliminating the problem previously discussed and of improving the electrical corrosion test as an evaluation tool in the development and use of fuel elements.

A. Electrical Chucking

Solutions to the problem of long time running without hot end chuck arcing are being actively pursued. A cutaway of the present hot end chuck design is shown in Figure 10a. The electrical chuck proper is the snout-like devide protruding to the left in the picture. The end of the test element is a sliding fit in the initial 1-1/4-inch opening in this snout. The enlarged section immediately behind the initial opening holds axial spacing blocks and a lobe holder for the purpose of testing a lobe section of a reactor

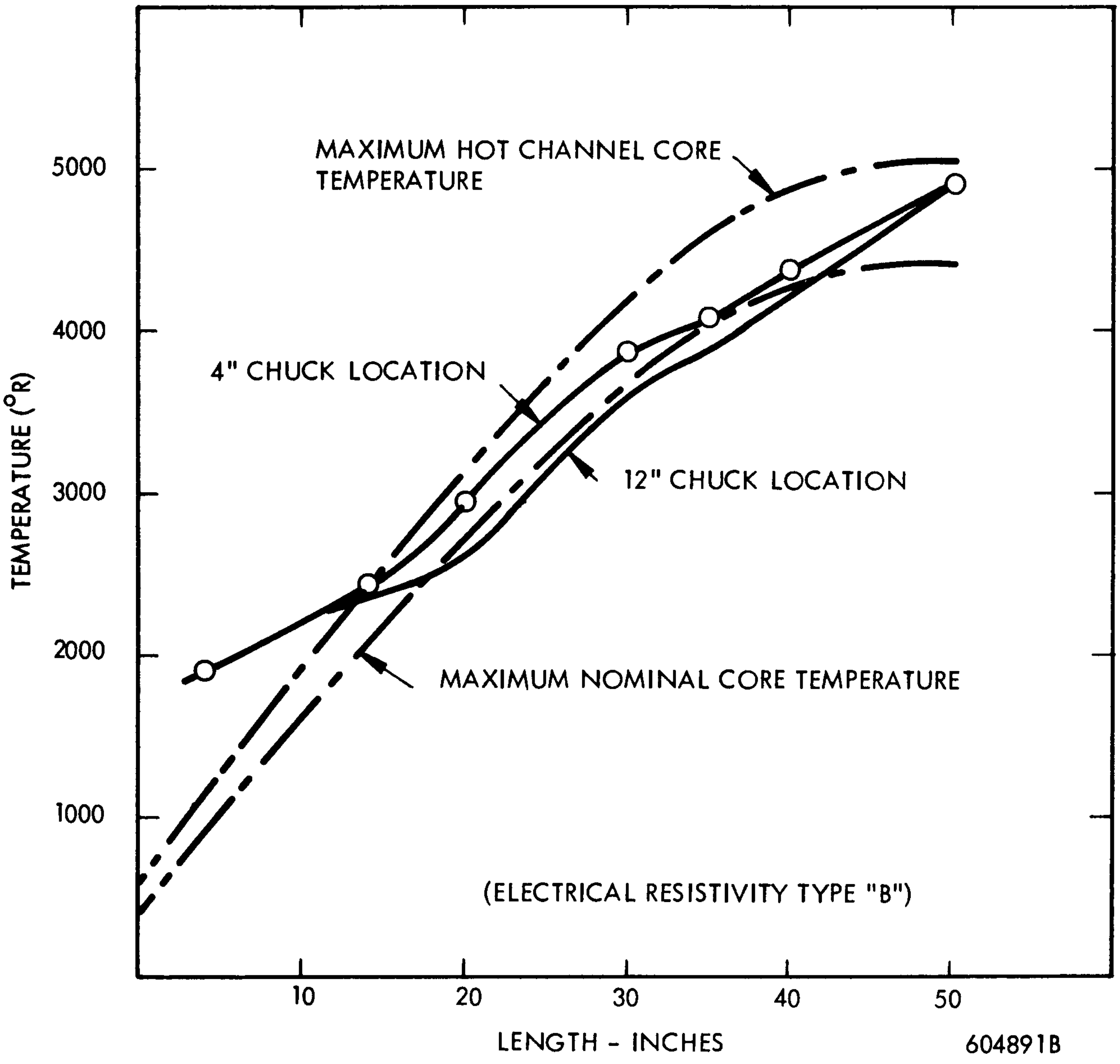

Figure 9

Chuck Position vs Maximum Material Temperatures

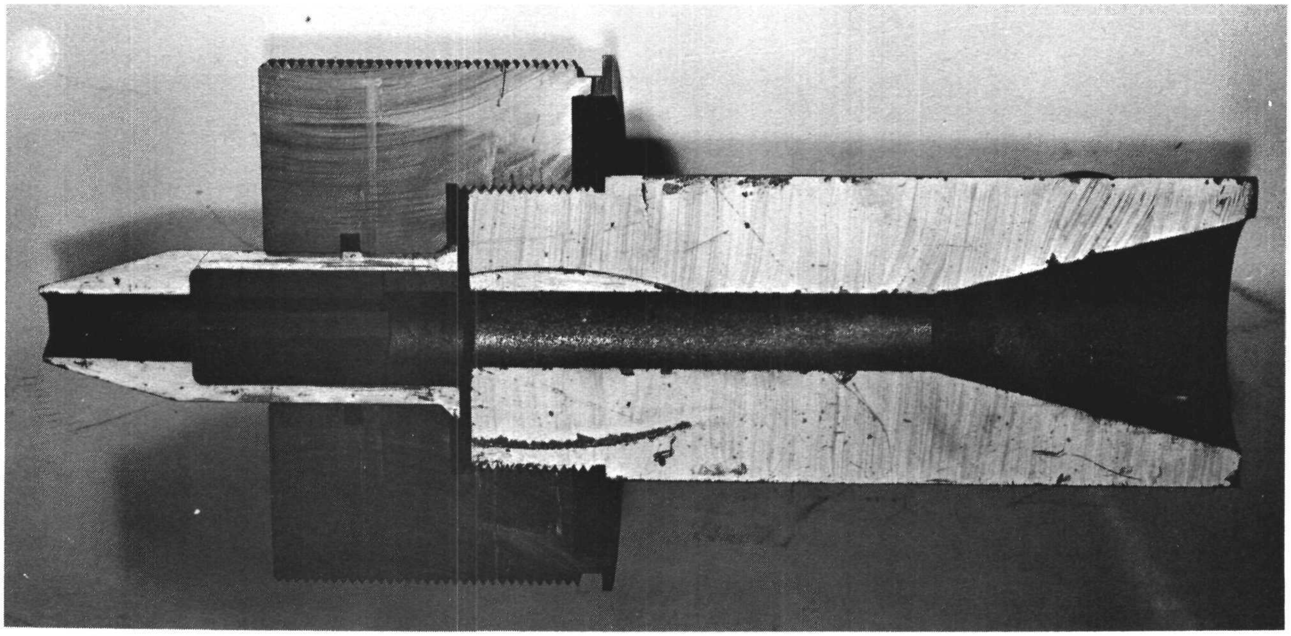

Figure 10a

Present Hot End Chuck Configuration - Sectioned support block. The test gas flow is from left to right in the picture. After passing through the chuck and its end pieces, the gas exits through the diffuser at the right. An external view of the chuck is shown in Figure 10b.

As can be seen from these previous figures, there is no positive means employed to make sure the chuck and element surfaces are in good electrical contact when changes in dimensions occur in those parts under test. To change this condition several new designs using spring or pressure loaded fingers have been tested and show electrical promise. Examples of two such designs are shown in Figures 11a, 11b and 12.

Clamping the element firmly on the hot end requires changes in the cold end chuck design to provide for relative thermal expansion and installation of the element. The current cold end chuck is a split finger design as shown in Figure 13a and clamps firmly on the cold end of the element. Two alternative cold end chuck designs which have been tried (with indifferent success) are shown in Figures 13b and 13c. Added work is required here and new designs are being prepared.

Another problem with the fingered or moveable segment hot end chucks is to reduce helium leakage to the level attainable with single piece chucks. Several design solutions are being readied for test. In the event these do not provide a solution, an alternate approach is a helium gland system on the cold end of the furnace. The helium pressure in the furnace chamber could then be dropped to slightly above the element exit pressure instead of being held at inlet pressure as is the current practice. *

---

*This might result in excessive hydrogen flow radially out through the pores of the element and such a system would have to be checked thoroughly for this possible side effect.

Figure 10b

Present Hot End Chuck - External View

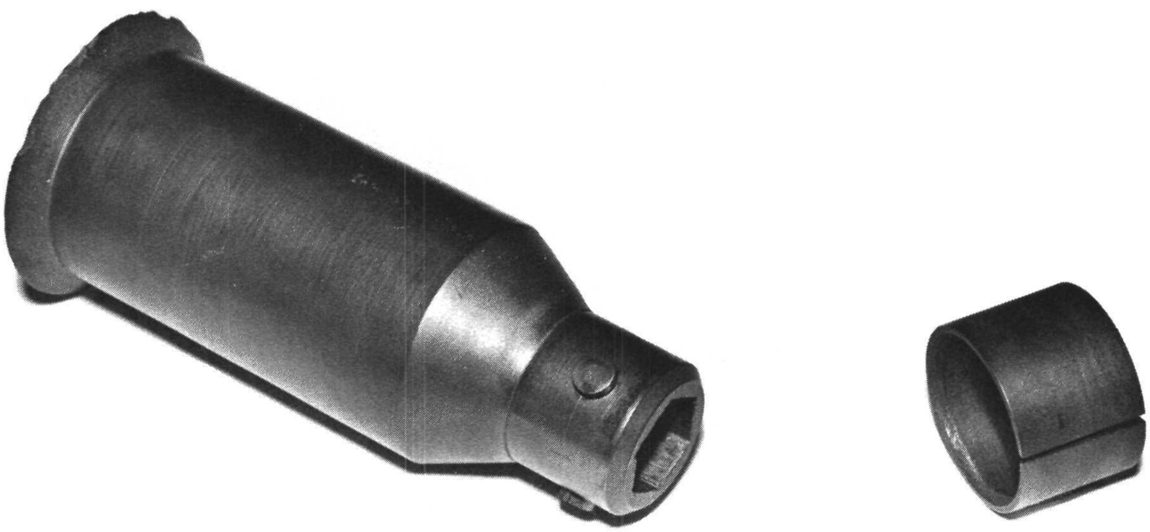

Figure 11a

Experimental Hot End Chuck – 3 Plunger Type – Snapring Removed

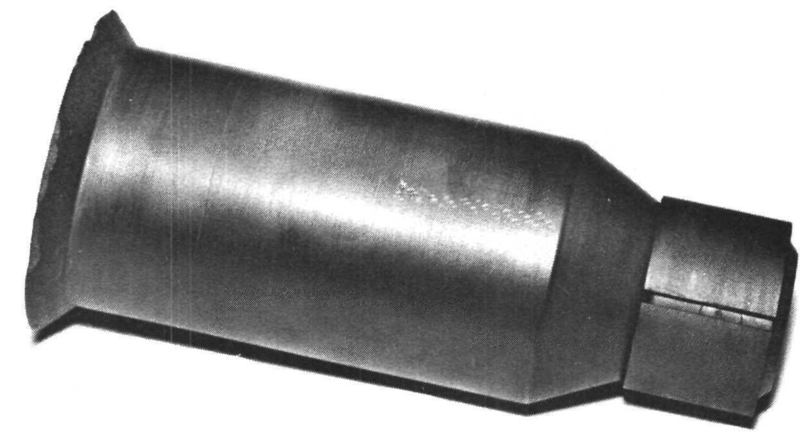

Figure 11b

Experimental Hot End Chuck - 3 Plunger Type - Snapring in Place

Figure 12

Experimental Hot End Chuck - Multifingered Type, External View

CONFIDENTIAL
RESTRICTED DATA
Atomic Energy Act - 1954

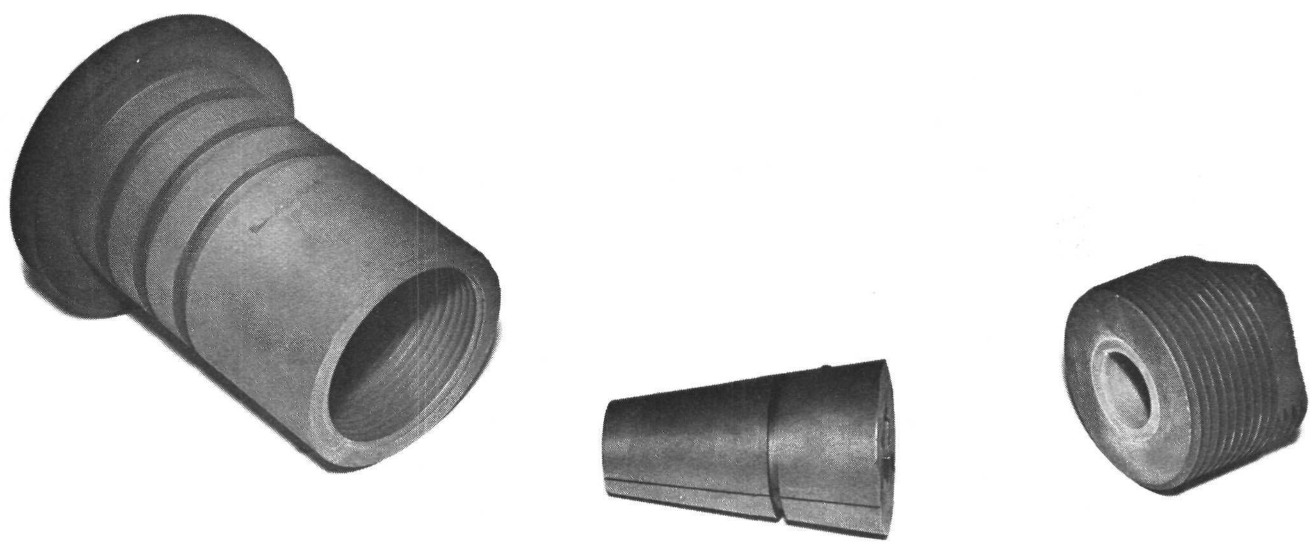

Figure 13a

Present Cold End Chuck, External View

CONFIDENTIAL
RESTRICTED DATA
Atomic Energy Act - 1954

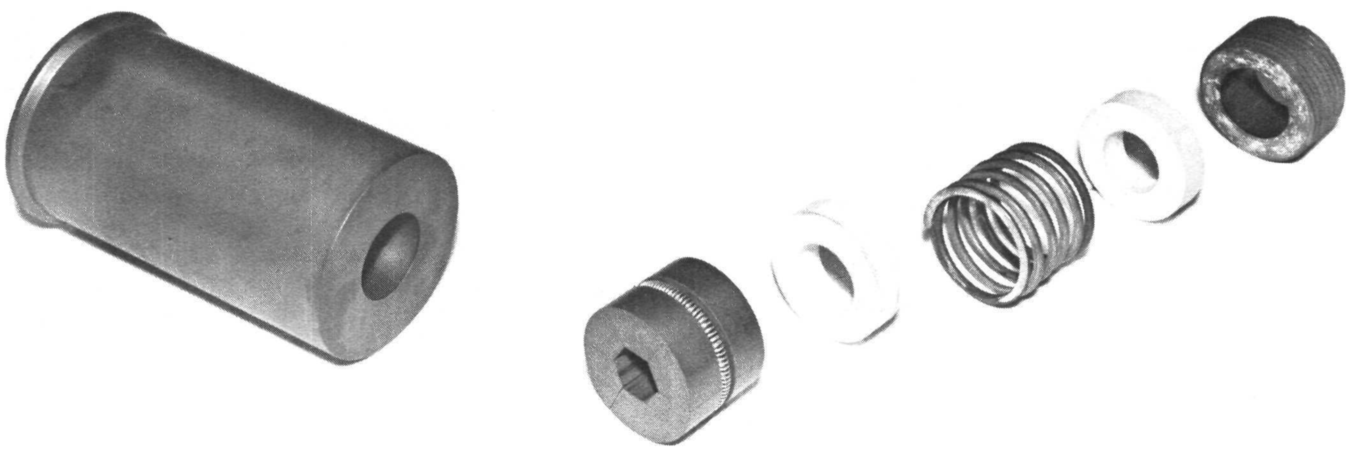

Figure 13b

Experimental Cold End Chuck - Split Cylinder Type

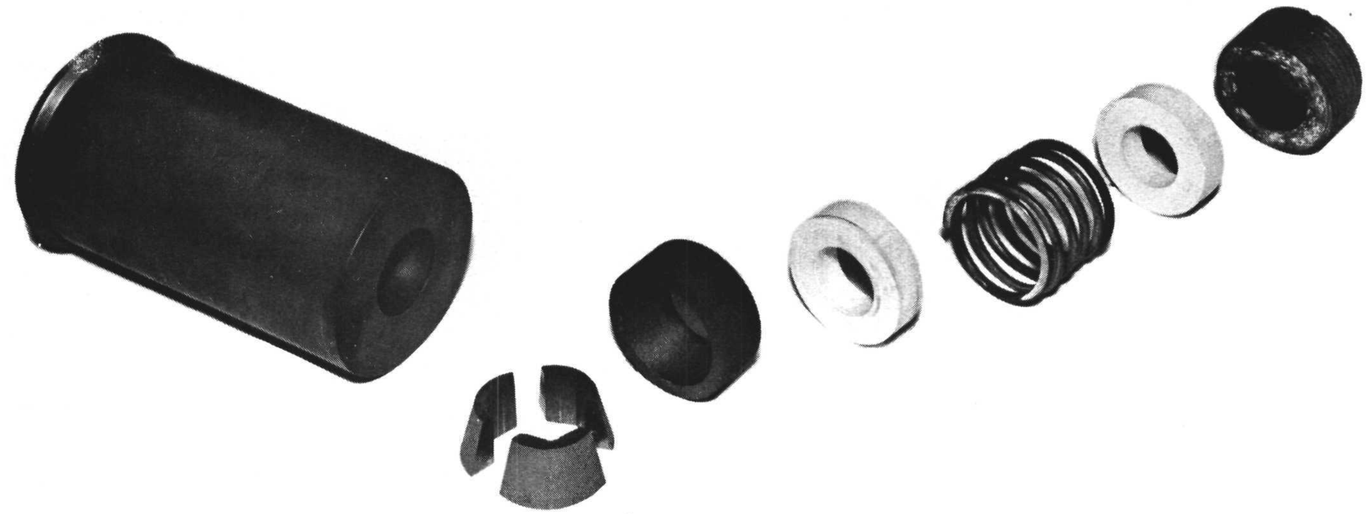

Figure 13c

Experimental Cold End Chuck - Split Cone Type

Another area of electrical chuck parametering has been discussed previously. This is the movement of the position of the cold end chuck axially along the element towards the hot end as a means of better simulating reactor-like temperature profiles. Pictures of three such extension pieces are shown in Figure 13d.

B. Radiation Shielding

On the basis of calculation, improved radiation shielding appears to be a way of controlling the test element radial temperature gradient up to surface temperatures of $5130^{o}R$. This is $500^{o}R$ above the present 1A test condition. Such an approach is substantially simpler to implement than one using guard heaters.

A conceptual design examination indicates that the element surface radiation loss can be reduced to about 1/4 of the unshielded rate. Such a design would consist of replacing the present 3 graphite shields with shields of 10 mil molybdenum. The emittance of molybdenum is approximately 3/8 that of graphite. In addition the inner most shield would be reduced to 2-1/2-inches inside diameter (from 4-inches) and the succeeding shields spaced successive quarter inches away. This whole assembly would be supported by very light-weight end shields.

On the basis of a reduction of the surface loss to 1/4 the unshielded rate, the radial temperature difference maximum to surface would be about $150^{o}R$ for a $5130^{o}R$ surface temperature. If for conservatism, the radiation losses are assumed increased to 1/2 the unshielded value, the radial temperature difference increases to about $485^{o}R$. This is about current practice. In this event some improvement could be obtained by orificing the outermost holes in an element with respect to the innermost as is done by LASL.[3]

Figure 13d

Experimental Cold End Chuck - Extension Pieces

C. Radiation Guard Heaters

An alternate approach to the control of an electrical test element's radial temperature gradient is the radiation guard heater. This approach, although more difficult to implement than a replacement of shielding, may in the end prove more satisfactory; either because of the added flexibility of an independent heat source* or because of the better life of relative thick graphite sections compared to thin refractory metal sheets with minimal support.

A guard heater with a separate power supply was studied first. On the basis of a fuel element and guard heater temperature distribution shown in Figure 14, calculations for a two-inch outside diameter, 22-inch long (covering the hot end only) heater gave a 240 KW maximum power requirement. (The fuel element temperature distribution chosen for these calculations is higher than that expected for the operation of NRX-A3 to A5 reactors, but it is in line with the maximum fuel element internal temperatures now encountered during environmental testing without a guard heater and it is also at a level that might be expected for the operation of more advanced reactors.) With proper modification of shield designs, the power requirement can be reduced to 120 KW. A separate power supply for this large a requirement is not now available in the test area.

A conceptual heater design for an independent power source is shown in Figure 15. The electrical connections can be mounted through any one of the five unused view ports. The use of such a heater will require modification of the existing radiation shields.

---

*Can be used to influence bulk material to bulk fluid temperature difference as well as element external surface to interior temperature difference.

[redacted]

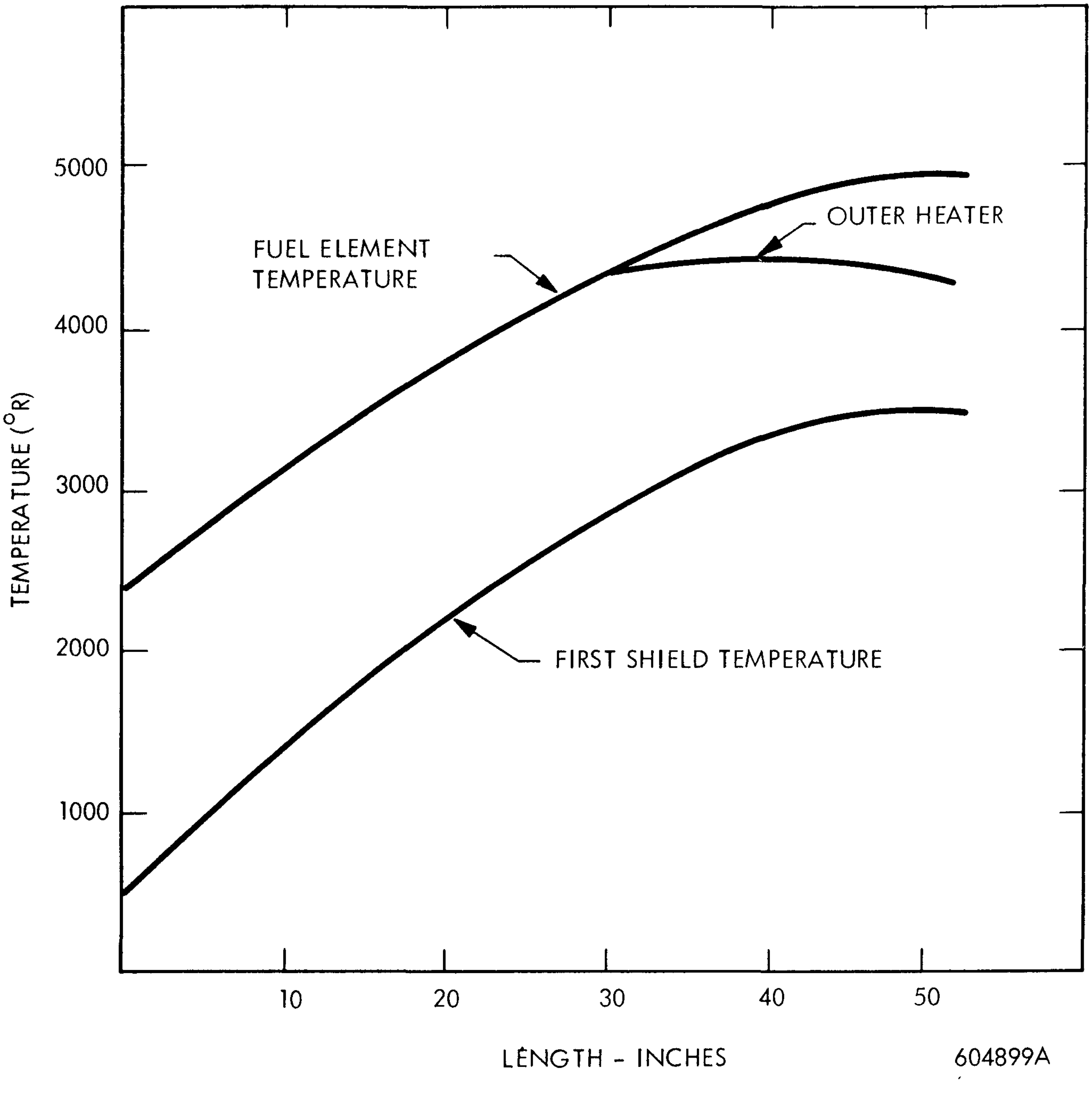

Figure 14

Guard Heater, Fuel Element Temperature

[redacted]

[redacted]

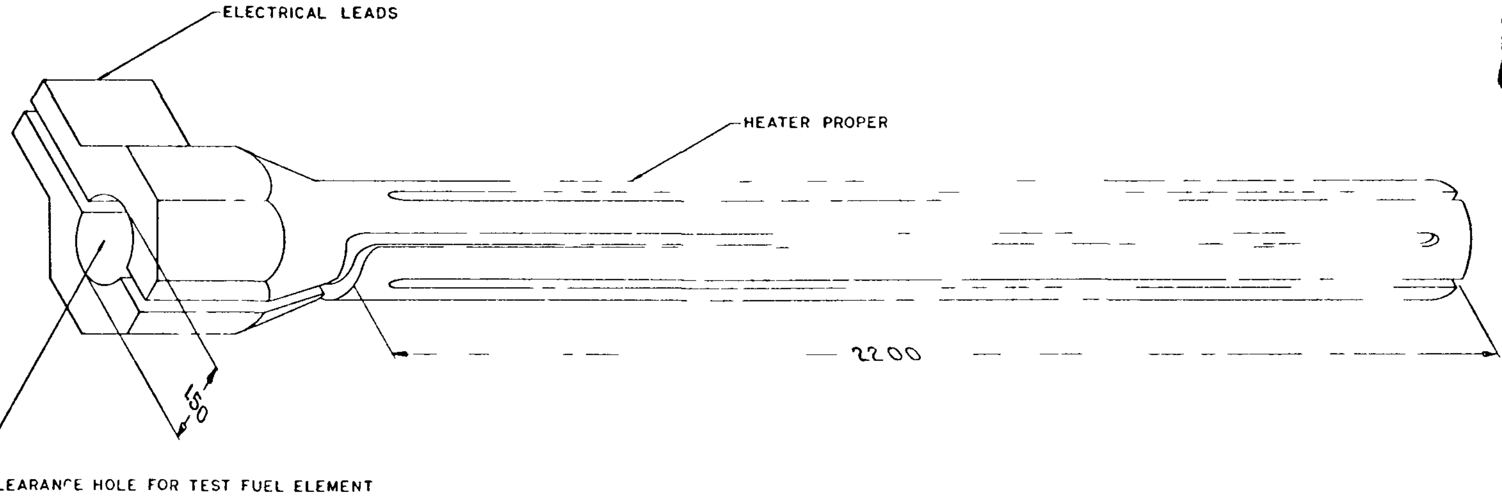

FIG 15 - CONCEPTUAL GUARD HEATER DESIGN SEPARATE POWER SUPPLY

Figure 15

Conceptual Guard Heater Design - Separate Power Supply

Astronuclear Laboratory

WANL-TME-1193

The more optimistic 120 KW guard heater power estimate can be satisfied by a current of 5000 amps with a 24 volt drop. A 5000 amp current is of the same order of magnitude as that through the test element, and in fact, a match in current requirements between the two can be designed into the guard heater. This plus the guard heater voltage drop requirement suggest that the heater and test element can use a common power supply if the heater is placed in series with the fuel element. A possible design scheme is shown in Figure 16.

The guard heater consists of concentric tubes with slots* cut through each to provide the desired heat generation rates. The guard heater and the existing chuck holder forms one single piece. Because the fuel element is now moved further downstream, a modified diffuser is required. The new diffuser should be so designed as to permit the accommodation of the support block holder.

The pyrographite insulations serve the following purposes:

1) reduce conduction losses, and
2) channel the current through the guard heater.

The dimensions of the heater as given is based on one that is coated with niobium carbide. The coating is recommended for two reasons:

1) it permits the testing of external corrosion of the fuel elements, and,
2) it reduces the radiation losses from the heater.

---

*The inner cylinder is slotted all the way to the hot end in order to provide proper contact of all surfaces.

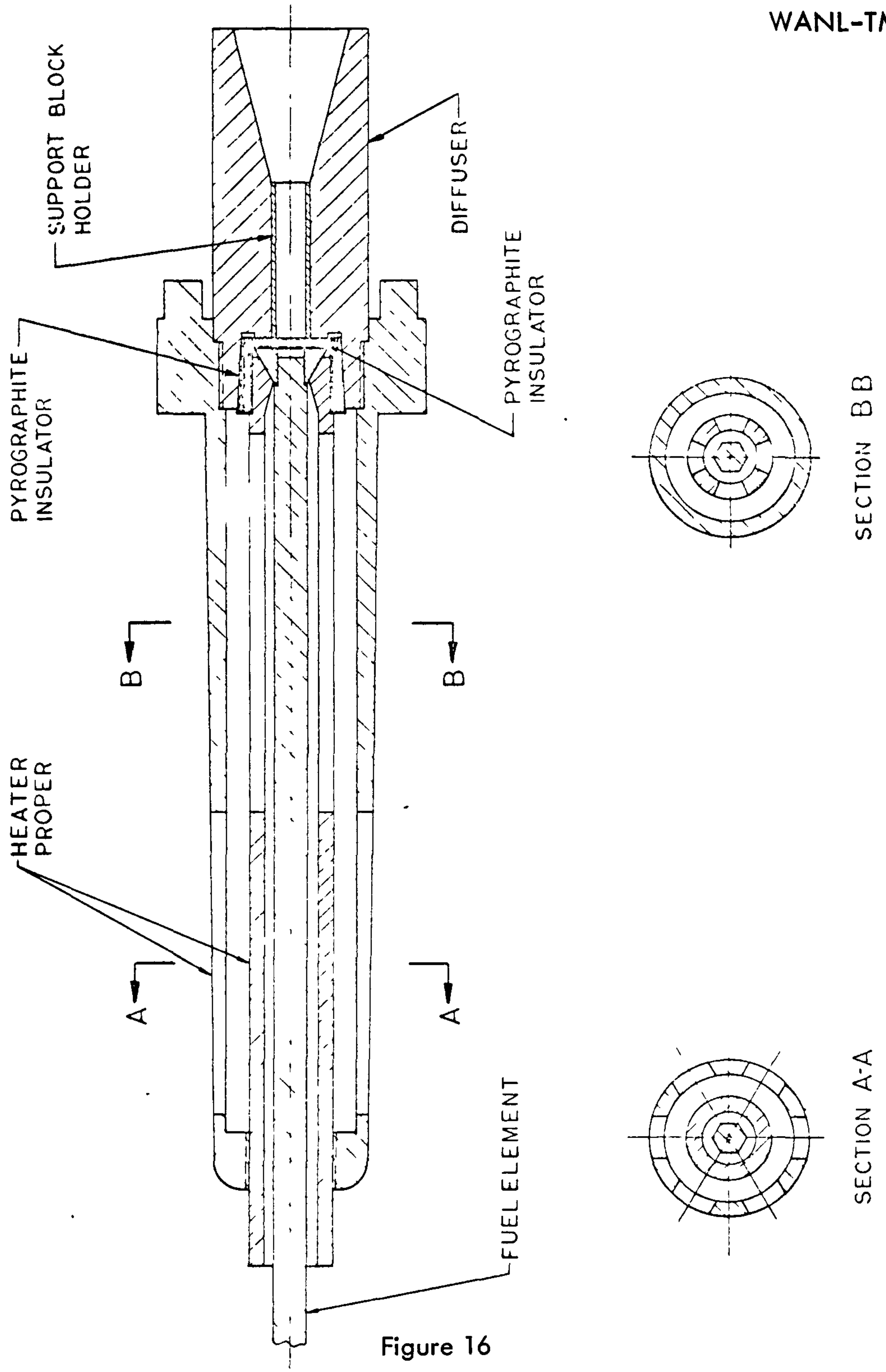

Figure 16

Conceptual Guard Heater Design - Element Power Supply

~~CONFIDENTIAL~~
~~RESTRICTED DATA~~
~~Atomic Energy Act 1954~~

The first graphite shield also needs modification to reduce heat losses. Two possible approaches are:

1) coat the surface with NbC, and
2) wrap the shield with pyrofoils.

Reducing radiation losses from the guard heater reduces power requirements and permits a thicker walled heater design. Thick walls are desirable because of the length of the heater and its fragility.

D. Additional Measurements

As has been brought out in the discussion in Section II-B, two important needs for additional test measurements are: (1) surface temperatures in the 20-inches to 30-inches axial length in location of the test element, and (2) a more accurate knowledge of the local electrical resistance of the test elements as a function of axial station.

Additional axial temperatures will be obtained by making use of currently unused view ports in the furnace body to take pyrometer readings on the element surface. In most of the A-2 furnace installations, viewing through these unused ports from the control room is more difficult than for the ports currently in use. Time and effort, however, should allow establishment of an adequate prism system to see around the various obstructions to direct sight.

The local resistance of an element under test can be determined by measuring the voltage drops along the element as a function of axial station at a constant value of test current. The voltage readings can be made by pressing or attaching electrical leads to the test element at periodic intervals. Potential differences between leads can then be balanced out through potentiometer circuits and readings taken without drawing current from the element.

Maintaining good electrical contact with the element without disturbing or damaging it and arcing from the leads to the furnace body are the chief developmental problems anticipated.

The temperature of the gas existing from electrical test elements is not now measured because of the difficulties involved. This is an obviously desirable measurement and work to obtain instrumentation to accomplish this is underway. The first approach is through use of the double sonic orifice aspirating temperature (Blockshear) probe concept. One metallic water-cooled model has already been tested in an A-2 furnace but failed from overtemperature of its parts. A redesign substituting uncooled coated graphite for the parts exposed to high temperatures is under construction for testing. Maintenance of the probe calibration because of changes in the first (high temperature) orifice's area with time may prove a development problem. Other ways in which this temperature might be measured, but for which no plans have been developed, are: (1) a well shielded button used as a pyrometer target, and (2) samples of graphite with corrosion rates known as a function of temperature in flowing hydrogen.

IV. FURNACE OPERATION TO 6000°R

Since the furnace has never been operated to this level, statements about its capability must be inferred from the design and current operating experience. One area of certainty is that current problems will not be improved by operating at higher temperatures. For example, maintaining a minimum radial gradient in the element becomes even more of a problem. The passive means of controlling surface heat loss do not look promising at these temperatures. An active means such as a guard heater surrounding the element appear required for control.

A problem from the past is likely to re-appear. This is arcing from the element or cold end electrode to the furnace body. To obtain the 6000°R temperature level, given the resistance characteristic of a test element, will require a substantial boost in voltage. In the past whenever the voltage drop over the furnace has exceeded 250 volts, arcing has been a problem. Since the furnace was last run at this 250 volt level, changes in electrical insulation, electrical hookup and maintenance procedures have been instituted which may have solved this problem.

A bright spot in the use of the A-2 furnace design at much higher temperatures is that the present furnace body will have structural integrity and adequate cooling. (Assuming the same exit pressure level and gas flow as is currently used.)

V. AUXILIARY EQUIPMENT CAPABILITY

A. Hydrogen Supply

In order to extend the capability of fuel element evaluations, in terms of time and temperature levels the gas supplies and the equipment now available must be considered. The gas supply currently in use consist of "Jumbo" trailers having a capacity of approximately 100,000 SCF of which 70,000 SCF can be used. Since the normal flow for evaluating elements is 500 SCFM, a continuous test duration of two (2) hours can be obtained from each trailer. Some difficulty has been experienced during extremely high test rates in obtaining sufficient trailers to supply our needs. The vaporizing system presently being installed will contain a storage capacity of 68,000 SCF operating as the accumulator for a 15,000 SCFH "Cryosonics" vaporizer. At present there are two 500 gallon liquid hydrogen storage dewars on hand, the equivalent of 120,000 SCF, which will provide an operating time of four (4) hours. The Waltz Mill Facility with its 90,000 SCF accumulator, 70,000 SCFH Linde vaporizer and 2700 gallon liquid hydrogen storage dewar is the more logical location of long time tests as it has a total volumetric equivalent of the dewar storage capacity of 320,000 SCF, or 12 hours operating time. Delivery schedules of either gas or liquid hydrogen will continue to be a problem.

B. Cooling Water Supply

The cooling water supply appears adequate to about 5500°R condition. At the extreme 6000°R condition, additional pumping capacity and a cooling tower may be required.

C. Power Supply

The total capacity of the power supply is adequate to the 6000°R condition. It is felt that by clever design the characteristics of the power supply can be matched to the furnace requirements through 6000°R.

D. Exhaust Gas Transition Piece and Heat Exchanger

Both of these pieces of equipment are marginal at the present time. Additional heat exchanger capacity is desirable. To take care of a 500°R increase in temperature, a small heat exchanger can be added without much trouble. More elaborate system changes will be required to achieve any greater increase in operating temperature.

E. Instrumentation and Controls

No substantial revamping of the control circuitry is required.

The present pyrometer is limited in range to 5500°R and the corrections used about 4400°R are an extrapolation of the "bulb" calibration below that level.

Operation at higher temperature levels will require correction of these deficiencies.

VI. CONCLUSIONS AND RECOMMENDATIONS

A major operational problem in the A-2 (single element electrical hydrogen corrosion test) furnace is that of arcing between the hot end electrode and the test fuel element. Other operational problems are (a) marginal exhaust gas heat exchanger and transition piece capacity, (b) occasional arcing between the electrically hot, thermally cold, end of the furnace to ground, and (c) the slow cooldown rate of the furnace. Aside from these difficulties, the furnace and its auxiliary equipment (hydrogen, water, power supply, etc.) appear adequate to substantially higher test temperatures than are currently used.

As approaches to operational problem solutions it is recommended that (1) the current program of electrical chuck experimentation be continued until the arcing from chuck to test element is eliminated as a source of difficulty, and (2) that exhaust gas heat exchangers and transition pieces of adequate thermal capacity be procured.

Simulation of reactor-like axial temperature distributions in the electrical test is better than might at first be expected but improvement is still desirable. A graphitization process has gone on in the hot end of past elements under test in such a way as to lower the electrical resistivity of the hot end with respect to the cooler portions of the test element. This reduces the electrical heat generation rate in the hot end in comparison to that in the cooler sections.

Substantial radial gradients exist in the electrical test specimen at the hot end compared to actual reactor-like conditions. It is felt that both improved radiation shielding and guard heaters can be used to control this radial temperature gradient. The guard heater offers superior control possibilities at present and modestly higher temperatures (+500°R) and is a necessity at even higher levels.

Substantial improvement of "goodness of fit" of electrical test axial temperature distributions to reactor-like distributions over the middle portion of the element can be obtained by varying the cold end chuck location with respect to the cold end of the element.

It is recommended that the uncertainties about the electrical tests axial temperature distribution be reduced by taking measurements of voltage along the element under test, increasing the number of element surface temperature measurements, and incorporating a means of measuring the elements exhaust gas temperatures.

It is recommended that the conceptual designs for improved radiation shielding and guard heating be firmed up and tried in actual operation as means of controlling the radial temperature gradient in the test element. Further it is recommended that a 1/2 megawatt power supply be procured to allow unimpeded implementation of the guard heater approach.

It is recommended that the program of varying the location of the cold end chuck with respect to the test element be continued.

VII. REFERENCES

1. WANL-TME-897, "Effect of Electrical Resistivity Variations on Maximum Material Temperatures During Environmental Testing of NRX-A2 Fuel Elements," J. W. H. Chi, September 29, 1964.

2. WANL-PR(J)-036, "Progress Report - October 1 through December 21, 1964, NERVA Nuclear Subsystem," January 25, 1965.

3. LA-3212-MS, "Quarterly Status Report LASL Rover Program for Period Ending November 30, 1964," Los Alamos Scientific Laboratory.

4. Glasser and Walker, "Thermal Imaging Techniques," Pg. 135; Plenum Press, 1964.

5. WANL-TME-840A, Volume 2, Reactor Analysis Data Book.

6. WANL-TME-744, "Thermal Analysis of High Temperature Fuel Element Corrosion Tests."

VII. APPENDIX A - DISCUSSION OF RADIANT HEAT TRANSFER ASSUMPTIONS

A. Radiation Interchange Factors

In examining the effects of shielding changes on the fuel element radiative heat loss, the usual grey body equation was used:

$$q_{1 \rightarrow 2} = A_1 \, F_{1 \rightarrow 2} \, \sigma \left(T_1^4 - T_2^4\right) \tag{1}$$

where

$q_{1 \rightarrow 2}$	is the net energy exchanged
A_1	is the area of the hotter surface
$F_{1 \rightarrow 2}$	is the radiation interchange factor
σ	is the Stefan-Boltzmann constant
T_1	is the hotter surface temperature
T_2	is the cooler surface temperature

If the fuel element and its surrounding shields are assumed to approximate coaxial cylinders of infinite length at uniform temperatures the radiation interchange factor is given by:

$$F_{1 \rightarrow 2} = \frac{1}{\dfrac{1}{\epsilon_1} + \dfrac{A_1}{A_2}\left(\dfrac{1}{\epsilon_2} - 1\right)} \tag{2}$$

where the undefined symbols are

ϵ_1	emissivity of the hotter surface
ϵ_2	emissivity of the cooler surface
A_2	area of the cooler surface

Quite obviously the real situation is that of finite length parts with substantial axial gradients. The magnitude of the errors introduced can be approximated by investigating two relatively simple situations where closed form solutions are easily obtained.

The first has to do with the viewing distance interaction along the lengths of the cylinders. Assume a flat plate source mounted on the center-line of a pipe as pictured in Figure A1. The hemispherical radiation from the flat plate source (A_1) initially intercepted by the pipe walls in the (+) x direction is given by:

$$\frac{d^3 \psi_b}{N_b A_1} = R^3 \int_{x=0}^{x=L} \int_{\psi=0}^{\psi=\pi} \frac{\sin \psi \, d_x \, d\psi}{R^2 + x^2} \tag{3}$$

where $d^3\psi_b$ is the differential of radiation

N_b is the areal radiant intensity

and the other symbols are defined by Figure A1.

Equation (1) integrated is:

$$\frac{d \phi_b}{N_b A_1} = \frac{\frac{L}{R}}{1 + \left(\frac{L}{R}\right)^2} + \tan^{-1}\left(\frac{L}{R}\right) \tag{4}$$

Now if $L = \infty$, $\frac{d\psi_b}{N_b A_1} = \frac{\pi}{2}$ or the pipe will intercept all of that portion of the flat plates radiation available to it in the (+ x) direction. The fraction of this total intercepted in any finite length L is then:

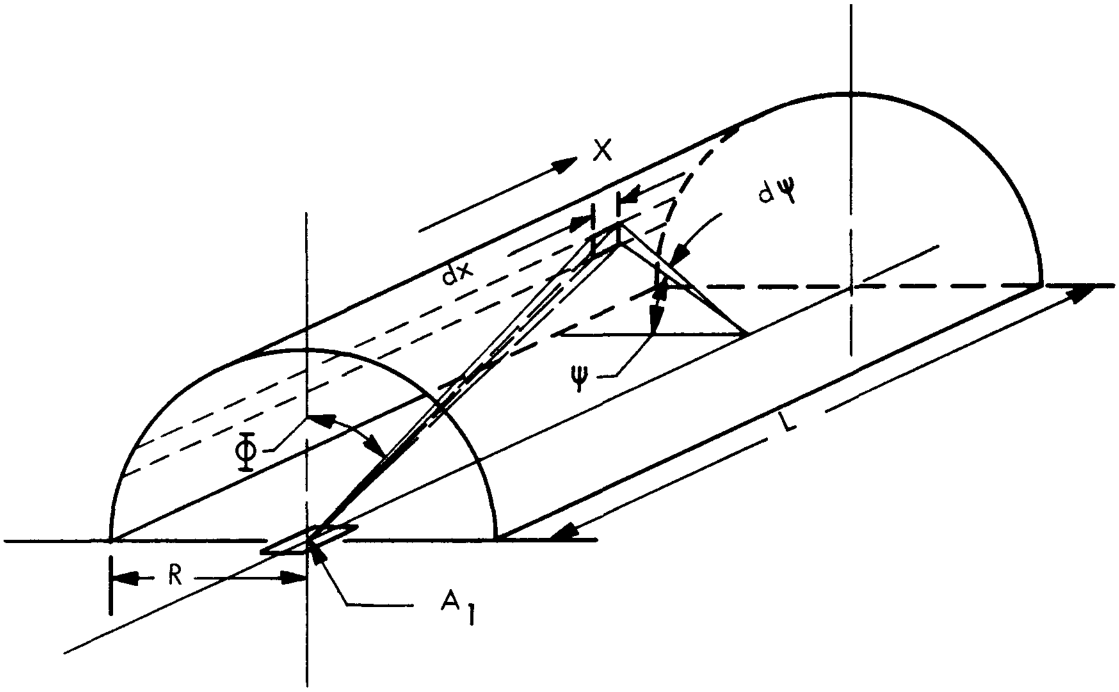

Figure A1

Diffuse Radiation From a Flat Plate on ℄ of a Pipe

$$\frac{\left[d\phi_b\right]_o^L}{\left[d\phi_b\right]_o^\infty} = \frac{2}{\pi}\left\{\frac{\frac{L}{R}}{1+\left(\frac{L}{R}\right)^2} + \tan^{-1}\frac{L}{R}\right\} \tag{5}$$

Numerically the comparison is shown in Table I:

$\frac{L}{R}$	$\left(d\phi_b\right)_L / \left(d\phi_b\right)_\infty$
0.5	0.55
1.0	0.82
2.0	0.96
3.0	0.99

Table I - Fraction of Hemisphical Radiation Intercepted by Pipe Wall

As can be seen almost all the radiation will be intercepted by the pipe in a length equivalent to three (3) times the radial distance between the emitting surface and the pipe. If the pipe is an adsorbing surface for the emitted radiation, Table I clearly indicates the lengthwise extent of the interchange. However, even if the pipe surface is a good diffuse (but not mirrorlike) reflector half the reflected radiation will be directed back in the general direction of its source and almost all of it will be re-intercepted by pipe surfaces and other source surfaces within the 6 radius length ($\pm$ 3 radius length) about the source. Of the other half, about 80% will be intercepted in and additional length equivalent to one radius. Thus with even a good diffuse reflector surface as the pipe or shield over 95% of the radiation exchange is within a length equivalent to $\pm$ 4 times the radial spacing between the emitting surface and the shield.

The question then resolves into how much difference in temperature between the ends of the $\pm$ 4 radius pipe length can be tolerated before the average temperature of the surfaces is not a reasonable index of the total radiation from the surfaces. To investigate this, assume that a surface has a linear temperature gradient from some temperature T_c at (+) 4 R length to some higher temperature T_h at (−) 4 R length so that the temperature at the midpoint (T_{av}) is the average of T_c and T_h. The ratio of the actual total radiation from the surface to that represented by the average temperature (T_{av}) would then be:

$$\frac{Q\,T_{av}}{Q_{actual}} = \frac{5}{16}\,\frac{\left[1+\frac{T_c}{T_h}\right]^4\left[1-\frac{T_c}{T_h}\right]}{\left[1-\left(\frac{T_c}{T_h}\right)^5\right]} \qquad (6)$$

A numerical comparison of $Q\,T_{av}/Q_{actual}$ as a function of T_c/T_h is given in Table II. As can be seen, radiation based on the average temperature is in good agreement with the actual when the coldest temperature is at least 3/4 of the hottest.

T_c/T_h	.5	.7	.75	.8	.9
$Q\,T_{av}/Q_{actual}$	.82	.94	.96	.98	.99

Table II - Comparison Between Average Temperature Radius and Actual Radiation With a Liner Temperature Gradient Along the Surface

Actual fuel elements are currently tested so as to reach maximum surface temperatures of about 4500°R with maximum temperature gradients of about 100°R/in along the element. A conclusion which can be drawn is that along the surface of the element at locations which are at least 4 radial spacing lengths* in from the element and shield ends, use of an infinite length, uniform temperature coaxial surface radiation interchange factor in calculations is reasonable if the spacing does not exceed 1-3/8-inches.

B. <u>Present Shield System Effectiveness</u>

The present A-2 furnace shield system consists of five concentric shields surrounding the test element. The three innermost shields are of graphite and the two outermost are of molybdenum sheet. These shields terminate at about the same point that the fuel elements enter the electrical chucks and no end shielding is used. In addition the radial distance between the surface of the element and the first shield is 1-5/8-inches. Under these circumstances calculation of radiative heat loss from the element surface cannot be reasonably approximated using the "infinite length" interchange factor (F) for enclosed cylinders (see Section 1 for this Appendix A).

---

*Near the element ends the "infinite length" factor will overstate the interchange by at least a factor of 2 unless end shielding is employed. Decreasing the radial spacing below 1-3/8-inches will obviously increase the portion of element length which is accurately assessed by "infinite length" radiation factor.

For the foregoing reason where calculations were made using present shield system empirically derived factors obtained from experimental data were used.

Assuming that all the heat lost from the surface of the element by radiation is transported away by means of the shield system, the heat loss from the element can be expressed as follows:

$$q_1 = \frac{\varphi_1 \left(T_1^4 - T_n^4\right)}{\left[1 + \varphi_1 \left(\frac{1}{\varphi_2} + \frac{1}{\varphi_3} + \cdots \frac{1}{\varphi_n}\right)\right]} \tag{7}$$

where q_1 is the net radiative heat transfer from the element surface at some location

$\varphi_1, \varphi_2 \cdots \varphi_n$ are the proportionality factors for heat exchange between the successive steps in the shield system including emissivity, view factors, conduction, etc.

T_1 is the element surface temperature at a particular location

T_n is the surface temperature of the n^{th} shield

The factor $\left[1 + \varphi_1 \left(\frac{1}{\varphi_2} + \frac{1}{\varphi_3} + \cdots \frac{1}{\varphi_n}\right)\right]$ can be evaluated for a particular set of experimental conditions from the expression:

$$\frac{1}{1 + \varphi_1 \left(\frac{1}{\varphi_2} + \frac{1}{\varphi_3} + \cdots \frac{1}{\varphi_n}\right)} = 1 - \left(\frac{T_2}{T_1}\right)^4 \tag{8}$$

where T_2 is the observed 1^{st} shield temperature

and the rest of the symbols have been previously defined.

A value derived from experimental data for the left hand expression of Equation (8) is 1/1.14. As this value is so close to 1.0, it will take a substantial shift in test conditions to make any effective change as far as calculations using the present shield system are concerned and the parameter has been treated as a constant.

Since there is no conduction (although some convection) between the test element and the 1^{st} shield, the proportionality factor $\wp_1$ can be approximated by the usual expression:

$$\wp_1 = A_1 F_{1 \rightarrow 2} \sigma \qquad (9)$$

where $F_{1 \rightarrow 2} = \epsilon_1$ for all practical purposes. That is for even the ideal infinite length, coaxial constant temperature (Equation (2)) case $F_{1 \rightarrow 2} \approx 0.99 \epsilon_1$.

C. Fuel Element Emissivity

A value of 0.95 was used as the fuel element surface emissivity in connection with the report. Emissivity of graphite surfaces is a strong function of the roughness of the surface but is largely independent of the wave length of the emitted radiation or the temperature of the emitter.[4] In the work reported in Reference 4, the emissivity of a highly polished surface was found to be 0.75. A deliberately roughened surface gave a value of 0.95. The highly polished surface measured 85-90% mirror like reflection. A comparison between the fuel element surface and the polished graphite surface of the hot end electrical chuck is given visually in Figure A2. As can be seen, the fuel element is quite dull in comparison. In addition thermal brightness measurements have been made on the element surface after locally roughening beyond the "as received condition" and compared to "as received" brightness. No difference could be determined. It is therefore assumed that the fuel elements are at the upper range of graphite emissivity.

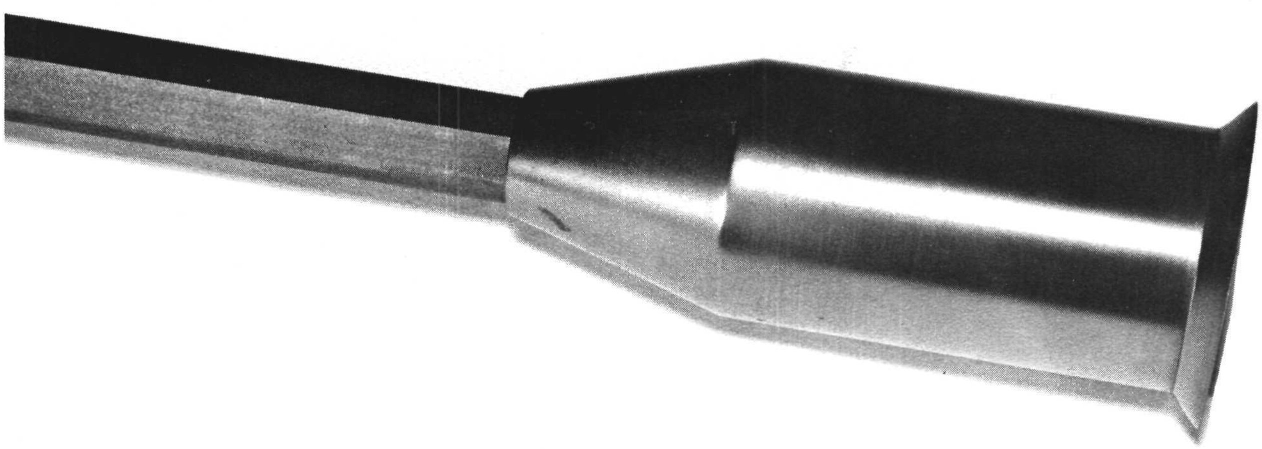

Figure A2

Comparison Chuck and Fuel Element Reflectivity